Tetrahedron 70 (2014) 2015–2019

Contents lists available at ScienceDirect

Tetrahedron

journal homepage: www.elsevier.com/locate/tet

A carbazole–oxadiazole diad molecule for single-emitting-component white organic light-emitting devices (WOLEDs)

Xiaoming Wu [a,*], Li Wang [a], Yulin Hua [a], Changsheng Wang [b], Andrei S. Batsanov [b], Martin R. Bryce [b,*]

[a] School of Materials Science and Engineering, Tianjin University of Technology, Tianjin 300384, PR China
[b] Department of Chemistry, Durham University, Durham DH1 3LE, UK

ARTICLE INFO

Article history:
Received 5 November 2013
Received in revised form 15 January 2014
Accepted 27 January 2014
Available online 1 February 2014

Keywords:
Carbazole
Oxadiazole
Fluorescence
Donor–acceptor system
Organic light-emitting device

ABSTRACT

The synthesis is reported of a new molecule consisting of *N*-phenylcarbazole linked through a butadiyne bridge to 2,5-diphenyl-1,3,4-oxadiazole. The compound shows blue photoluminescence with positive solvatochromism: e.g., λ_{max} 401 nm in cyclohexane, 461 nm in chloroform solution (quantum yield Φ_f 0.55) and 428 nm in thin film, with a low intensity band extending to ca. 700 nm in films. OLEDs with a device configuration of [ITO/PEDOT:PSS (50 nm)/molecule:PVK:OXD-7 (80 nm)/Bphen (20 nm)/LiF (0.8 nm)/Al (120 nm)] were fabricated. Pure white-light emission with Commission Internationale De L'Eclairage (CIE) coordinates of (0.313, 0.330) at 13 V and good colour stability with a very small offset of coordinates (0.034, 0.033) under biases of 9–15 V has been achieved.

1. Introduction

The vast majority of organic materials that have been developed for organic light-emitting diodes (OLEDs)[1] emit monochromic light with a relatively narrow electroluminescent (EL) spectral band.[2] Therefore, the broad electroluminescence spectrum required for white light emission (WOLEDs)[3] is usually generated from the combined emission of three primary colours or two complementary colours in a complicated device architecture.[4–7] However, this approach is problematic because energy readily transfers from the higher energy to the lower energy dyes and careful adjustment of the concentration of each dye is required to achieve a balanced white emission colour. This energy transfer problem is partly mitigated if the dyes are segregated into different layers.[8] For example, Reineke et al. achieved fluorescent tube efficiencies of 81 lm W^{-1} at 1000 cd/m^2 using lens-based outcoupling (×2.7 enhancement) with three-component primary red, green and blue (RGB) phosphorescent emitters.[3a] It is easier to adjust the composition of a two-chromophore system and a more convenient way to obtain white emission is to use complementary blue and yellow/orange emitters.[9] WOLEDs have also been fabricated utilising multiple emissions from monomers and excimers or exciplexes.[10] Efficiencies of these devices are often low, although very recently a peak external quantum efficiency (EQE) of >20%, Commission Internationale De L'Eclairage (CIE) coordinates of (0.33, 0.33) and a colour rendering index (CRI) value of 80 has been reported for an excimer-based phosphorescent WOLED;[10f] these data are comparable to state-of-the-art WOLEDs with multiple dopants.

Single-component fluorescent emitters—small molecules and short oligomers[11] or polymers[12]—with a broad emission spectrum have only rarely been utilised in WOLEDs. A single white-emitting molecule offers the advantages of simplified processing, as well as avoiding differential aging of multiple emitters and morphological changes upon device operation that adversely affect colour stability.

We now report on the synthesis, photophysical characterisation and electroluminescence of the new fluorescent compound **4**. 'Pure' white light (CIE: 0.313, 0.330) with a high CRI of 84–88 has been achieved using **4** as a single-component emitter in WOLEDs. Compound **4** is a donor–acceptor system and is structurally very distinct from compounds used previously for WOLEDs.

2. Results and discussion

2.1. Molecular design, synthesis and characterisation

Carbazole (Cz)[13] and diaryl-1,3,4-oxadiazole (OXD)[14] are well known as thermally stable, hole- and electron-transporting

* Corresponding authors. E-mail addresses: wxm@mail.nankai.edu.cn (X. Wu), m.r.bryce@durham.ac.uk (M.R. Bryce).

0040-4020/$ – see front matter © 2014 Elsevier Ltd. All rights reserved.
http://dx.doi.org/10.1016/j.tet.2014.01.073

materials, respectively, and their derivatives have been widely used as emitter and/or charge-transport layers in OLEDs. Bipolar covalent Cz-OXD diad molecules have received attention as blue and green emitters[15] but they have not been used previously as white-light emitters. The novel feature of compound **4** is the incorporation of the rigid, conjugated butadiyne linker between the Cz and OXD units. The synthesis of **4** via Sonogashira cross-coupling of **2** and **3** is shown in Scheme 1. The key reagents **1**[16] and **3**[17] have been reported previously.

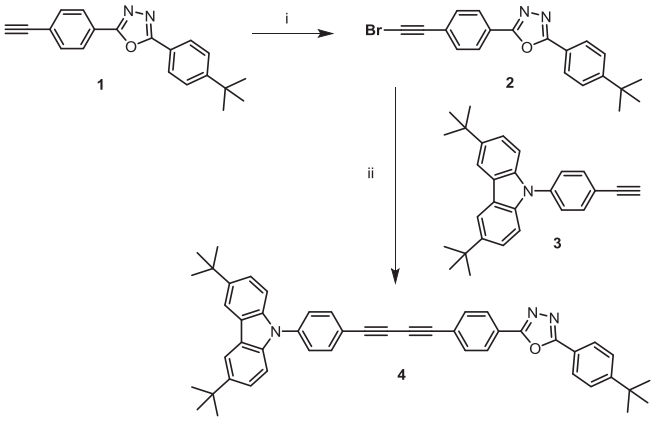

Scheme 1. Reagents, conditions and yields: i) *N*-bromosuccinimide, $AgNO_3$, acetone, 22 °C, 77% yield; ii) **3**, $Pd(PPh_3)_2Cl_2$, CuI, triethylamine, THF, 22 °C to 50 °C, 42% yield.

The structure of compound **4** was unambiguously established by NMR spectroscopy, mass spectrometry, elemental analysis and single-crystal X-ray crystallography of **4**·1/4 PhMe (Fig. 1). Moderately twisted diphenyloxadiazole moieties (*iii*–*iv*–*v*) form a slanted π–π stack with mean interplanar separations of ca. 3.6 Å, whereas effective stacking of carbazole moieties *i* is prevented by almost perpendicular orientation of the adjacent benzene ring *ii* (see SD for an additional figure).

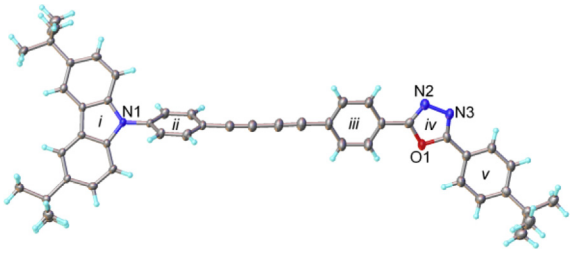

Fig. 1. X-ray molecular structure of **4**. Interplanar angles (°): *i*/*ii* 62.7, *ii*/*iii* 87.8, *iii*/*iv* 6.5, *iv*/*v* 11.1, *iii*/*v* 17.6.

2.2. Photophysical studies

Normalised absorption and photoluminescence spectra for compound **4** are shown in Fig. 2 and the data are collated in Table 1. The absorption spectra in cyclohexane, chloroform and thin film have very similar profiles with a strong band at ca. 340 nm and a lower intensity shoulder at ca. 375 nm. The main absorption features are attributed to π–π* transitions, following literature precedents for these types of compound.[18] Blue to green emissions are observed in solutions (λ_{max}: cyclohexane 401, chloroform 461, dichloromethane 487, acetonitrile 549 nm). The significant positive solvatochromism is consistent with dipolar interactions of the donor–π–acceptor molecule **4** with the polar solvent.[19] In the thin film state the λ_{max} of photoluminescence (428 nm) is located between that observed in non-polar and polar solvents. A similar shift in film emission, intermediate between non-polar and polar solvents, has been reported previously for dipolar carbazole derivatives.[20] For films of **4** a low intensity tail in the emission band extends to ca. 700 nm, which is not observed in the solution spectra. This has precedent in previous work and is generally ascribed to π-stacking of the molecules[20] and/or excimers in the film.[11c]

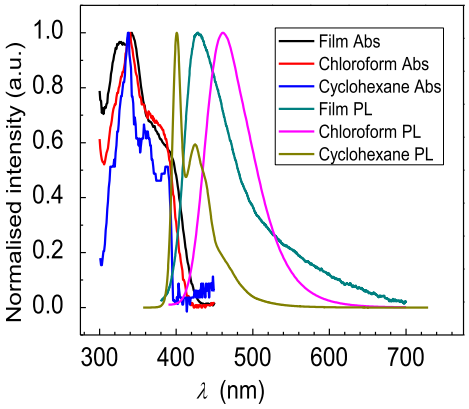

Fig. 2. UV–vis absorption and emission spectra for compound **4**.

For OLED studies (see below) poly(*N*-vinylcarbazole) (PVK) was used as the host material. Fig. 3 shows the transient photoluminescence decay curves for films of neat **4**, and **4** (3% by weight) blended in PVK. The decays are exponential with fluorescence lifetimes of 38.0 ns (neat film) and 51.5 ns (**4**:PVK). These data indicate that the quenching of excitons in the **4**:PVK blend film is significantly reduced, and partial energy transfer exists between the host and dopant.[21] Atomic force microscopy (AFM) images reveal that the **4**:PVK blend film has a lower surface roughness (Ra: 0.303) compared to the neat **4** film (Ra: 0.603) as shown in Fig. 4. The PVK should thus facilitate the transport of charge carriers at the interfaces of the emitter:PVK/transport layers in OLEDs.

2.3. Electroluminescence (EL) properties of OLEDs of 4

For OLED fabrication PVK was used as the host for the emitter, not only to enhance the EL performance but also to improve the film uniformity of the emitting layer assembled by spin-coating.[22] The device architecture used is: [ITO/PEDOT:PSS (50 nm)/**4**:PVK:OXD-7 (80 nm)/Bphen (20 nm)/LiF (0.8 nm)/Al (120 nm)]. For these devices, PEDOT:PSS is a hole transport layer (HTL); the emitting layer is PVK doped compound **4** and 1,3-bis[(4-*tert*-butylphenyl)-1,3,4-oxadiazolyl]phenylene (OXD-7); 4,7-diphenyl-1,10-phenanthroline (BPhen) serves as an additional electron transport layer adjacent to the LiF/Al cathode.

The EL spectra of the WOLED under biases of 9–15 V are illustrated in Fig. 5, with the two main peaks at λ_{max} ca. 450 and 575 nm corresponding to blue and orange-red emission. The peak width at half height covers a wide wavelength range of ca. 430–640 nm, which results in a high colour rendering index (CRI) of 84–88 for the white light emission. As the driving voltage is increased from 9 to 15 V, the higher energy emission band rises in relative intensity until ca. 12–14 V and then begins to reduce. On the contrary, the lower energy emission displays the opposite trend. Fig. 6 depicts the variation of CIE coordinates as the applied voltage varies from 9 to 15 V. The best coordinates of (0.313, 0.330) are achieved at 13 V and they locate very close to the equal-energy white point of (0.333, 0.333) with a very small offset of (0.034, 0.033) under the various biases. These data demonstrate that pure white emission and

Table 1
Photophysical data for **4**

Abs, cyclohexane, λ_{max}/nm (ε M^{-1} cm^{-1})	Abs, chloroform, λ_{max}/nm (ε M^{-1} cm^{-1})	Abs, thin film, λ_{max}/nm	Em, cyclohexane, λ_{max}/nm	Em, chloroform, λ_{max}/nm	Em, thin film, λ_{max}/nm
338 (1.77×10^5)	340 (2.19×10^5)	340	401; Φ_f 0.92	461; Φ_f 0.55	428

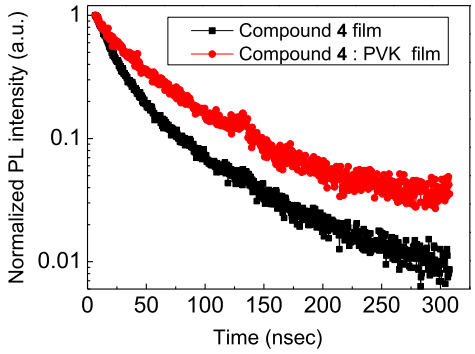

Fig. 3. Transient photoluminescence decays of a film of neat **4** (black) and **4** (3% by weight) blended in PVK film (red) at room temperature; λ_{exc} 340 nm.

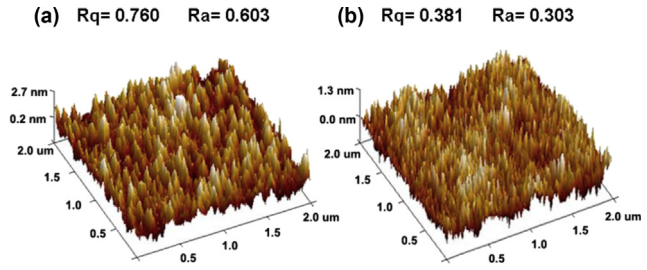

Fig. 4. Atomic force microscopy images of (a) ITO/compound **4** and (b) ITO/compound **4** (3% by weight) blended in PVK.

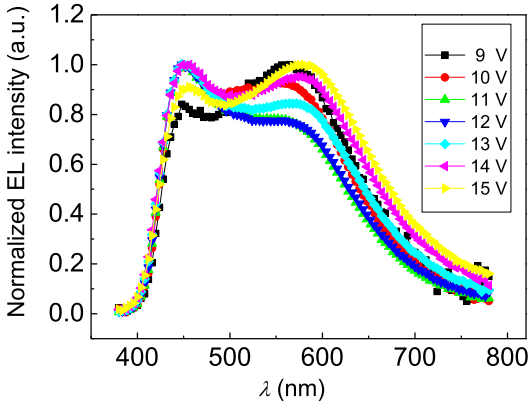

Fig. 5. Normalised EL spectra of the white OLEDs [ITO/PEDOT:PSS/**4**:PVK:OXD-7/Bphen/LiF/Al] under driving voltages of 9–15 V.

remarkably good colour stability have been achieved using compound **4**. These data also suggest that a balanced distribution of holes and electrons has been achieved within the recombination zone in the emitting layer. This could be facilitated by the donor–acceptor (bipolar) structure of the emitter.

Devices were initially fabricated without the addition of OXD-7 into the emitting layer (EML) and although pure white light could be achieved, the device exhibited only a relatively weak performance with a high turn-on voltage of 12 V at 1.8 cd/m^2, a maximum

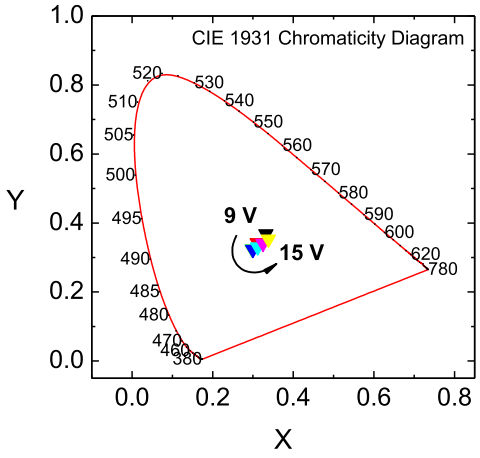

Fig. 6. The CIE chromaticity diagram at driving voltages of 9–15 V.

brightness of 32 cd/m^2 at 20 V, and a maximum current efficiency of 0.03 cd/A at 25.1 mA/cm^2. We rationalise this as follows. Holes transported from the PEDOT:PSS could be easily injected into the EML as the host PVK has hole transport character. However, the lowest occupied molecular orbital (LUMO) of PVK is 2.2 eV,[23] which is much higher than that of the ETL (Bphen) (2.9 eV).[24] Even with this ETL layer, the efficiency of electron injection into the EML will be low due to the high energy barrier of 0.7 eV between EML and ETL, which results in unbalanced charge carrier distribution in the EML. For this reason, OXD-7 with a lower LUMO of 3.0 eV,[25] was blended into the emitting layer to facilitate the electron injection from the ETL to EML via the lower energy barrier of 0.1 eV. The balance of the carriers is improved accordingly, which will result in an enhancement of the recombination rate for the hole–electron pairs. Based on this approach, the optimum WOLED presented a lower turn-on voltage of 8 V at 1.7 cd/m^2, and a maximum brightness of 116 cd/m^2 was achieved at 14.5 V, as shown in the current density–voltage–luminance (J–V–L) curves (Fig. 7). The device exhibited a maximum current efficiency of 0.12 cd/A at 12.5 mA/cm^2 (10 V) as shown in Fig. 8. The inset of Fig. 8 is a photograph of the WOLED at 10 V; pure white light emission with a uniform emitting area is seen.

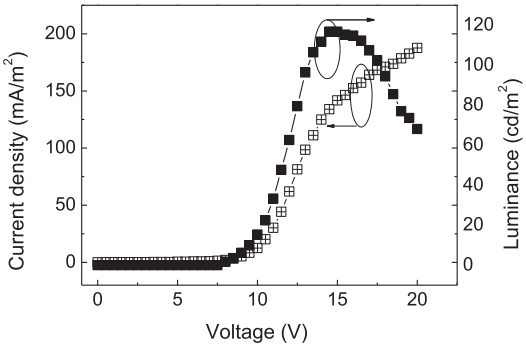

Fig. 7. The current density–voltage–luminance (J–V–L) curves of the white OLED.

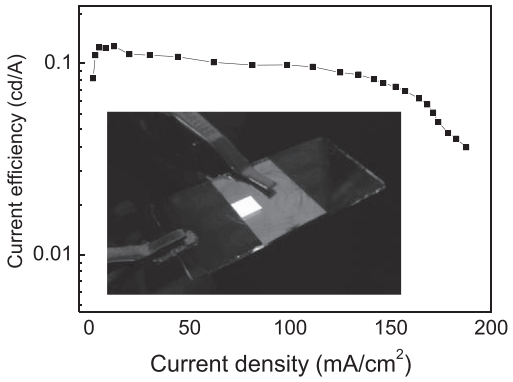

Fig. 8. The current efficiency–current density curve of the white OLED. Inset: a photograph of a WOLED operating at 10 V.

The strong orange-red emission band in the EL (Fig. 5), which is not observed in PL, is consistent with the formation of electric field induced electromers during device operation.[3d,11a,c,e] This lower energy band has not been observed in OLEDs of previous covalent Cz-OXD diad molecules, all of which have more twisted backbone structures than **4**. The molecular rigidity imparted by the butadiyne linkage in **4**, may, therefore, be a key molecular design feature for achieving white emission in this family of compounds.

3. Conclusions

The synthesis, characterisation and properties of **4** as a single-component WOLED fluorescent emitter have been described. The OLED presents a promising combination of 'pure' white-light emission with CIE coordinates of (0.313, 0.330) at 13 V and very good colour stability under the various applied biases. The corresponding high CRI value is in the range 84–88. To place this work in a broader context, devices based on compound **4** demonstrate a good trade-off between simple device architecture, efficiency, CRI and colour stability, with WOLED data that are comparable with recent values for other small-molecule single-component emitters.[11] Compound **4** is structurally very distinct from compounds used previously for white-light emission. Our future research will include systematic modifications to the chemical structure and detailed photophysical studies to provide further understanding of this interesting class of emitters.

4. Experimental section

4.1. General information

All reactions were conducted under a blanket of argon, which was dried by passage through a column of phosphorus pentoxide. All commercial chemicals were used without further purification. Anhydrous solvents were prepared using an Innovative Technology Inc. solvent purification system. Column chromatography was carried out using 40–60 μm mesh silica (Fluorochem). NMR spectra were recorded on: Bruker Avance-400, Varian VNMRS 700 and Varian Inova 500 spectrometers. Chemical shifts are reported in parts per million relative to tetramethylsilane (0.00 ppm). Melting points were determined in open-ended capillaries using a Stuart Scientific SMP40 melting point apparatus at a ramping rate of 2 °C/min. Mass spectra were measured on a Waters Xevo OTofMS with an ASAP probe. Elemental analyses were obtained on an Exeter Analytical Inc. CE-440 elemental analyser. IR spectra were recorded on a Perkin Elmer FT-IR Paragon 1000 spectrometer.

4.2. Synthesis of materials

*4.2.1. 2-(4-tert-Butylphenyl)-5-[4-(2-bromo-ethynyl)phenyl]-1,3,4-oxadiazole (**2**).* To the solution of 2-(4-*tert*-butylphenyl)-5-(4-ethynylphenyl)-1,3,4-oxadiazole (**1**)[16] (1.24 g, 4.1 mmol) in acetone (50 cm^3) was added *N*-bromosuccinimide (NBS) (0.80 g, 4.49 mmol) and silver nitrate (0.10 g, 5.9 mmol). The mixture was stirred at 22 °C for 1 h to yield a pale-yellow suspension. The precipitate was removed by suction filtration through a Celite pad and the filtrate was vacuum concentrated to dryness. The solid residue was recrystallised from ethanol to afford product **2** as off-white crystals (1.21 g, 77%). Elemental analysis (%) calcd for $C_{20}H_{17}BrN_2O$: C, 63.00; H, 4.49; N, 7.35. Found: C, 62.84; H, 4.46; N, 7.34. HR-MS (ASAP$^+$) *m*/*z* calcd for [M]$^+$ 380.0524, found *m*/*z*: 380.0526. ^{1}H NMR ($CDCl_3$, 400 MHz) δ=1.36 (s, 9H), 7.54 (d, *J* 8.8 Hz, 2H), 7.58 (d, *J* 8.8 Hz, 2H), 8.04 (d, *J* 8.4 Hz, 2H), 8.07 (d, *J* 8.8 Hz, 2H). ^{13}C NMR ($CDCl_3$, 100 MHz) δ=31.3, 35.3, 79.6, 121.1, 124.1, 126.2, 126.3, 126.9, 127.0, 132.8, 155.7, 164.0, 165.1.

*4.2.2. Compound **4**.* [4-(3,6-Di-*tert*-butyl-*N*-carbazolyl)]phenylacetylene (**3**)[17] (199 mg, 0.524 mmol), compound **2** (191 mg, 0.5 mmol), $Pd(PPh_3)_2Cl_2$ (15 mg, 0.02 mmol) and CuI (5 mg, 0.026 mmol) were mixed with dry THF (10 cm^3) and triethylamine (10 cm^3). The mixture was degassed by bubbling argon for 20 min then stirred at 22 °C for 12 h. The temperature was raised to 50 °C and the reaction was continued for an additional 2 h. The resultant yellow suspension was vacuum evaporated to dryness and the residue was column chromatographed on silica eluted with DCM–2% diethyl ether to yield a yellow solid. The solid was recrystallised from ethanol followed by a second recrystallisation from toluene–acetonitrile mixture to yield compound **4** as yellow crystals (142 mg, 42%). Elemental analysis (%) calcd for $C_{48}H_{45}N_3O$: C, 84.80; H, 6.67; N, 6.18. Found: C, 84.97; H, 6.71; N, 5.78. HR-MS (ASAP$^+$) *m*/*z* calcd for [M]$^+$ 679.3563, found *m*/*z*: 379.3566. ^{1}H NMR ($CDCl_3$, 500 MHz) δ=1.40 (s, 9H), 1.49 (s, 18H), 7.42 (d, *J* 8.5 Hz, 2H), 7.50 (dd, J_1 8.5 Hz, J_2 2.0 Hz, 2H), 7.58 (d, *J* 8.0 Hz, 2H), 7.60 (d, *J* 8.5 Hz, 2H), 7.72 (d, *J* 8.0 Hz, 2H), 7.77 (d, *J* 8.5 Hz, 2H), 8.09 (d, *J* 8.0 Hz, 2H), 8.16 (m 4H). ^{13}C NMR ($CDCl_3$, 125 MHz) δ=31.1, 32.0, 34.7, 35.1, 74.3, 76.7, 80.9, 82.5, 109.2, 116.3, 119.5, 120.8, 123.7, 123.8, 124.2, 125.0, 126.1, 126.2, 126.78, 126.82, 133.1, 134.0, 138.6, 139.3, 143.4, 155.6, 163.7, 164.9. IR (solid) ν 2957, 2182, 2160, 1600, 1515, 1488, 1456, 1294, 1265, 847, 809 cm^{-1}. X-ray crystal structure: CCDC number 956292.

4.3. Photophysical characterisation

Photoluminescence (PL) and absorption (Abs.) spectra of compound **4** dissolved in solvents were measured with a Hitachi F-4500 fluorescence spectrophotometer and a Hitachi U-4100 UV–vis–NIR spectrophotometer. The PL transient decay characteristics in films [film 1: compound **4** 2 wt % in $CHCl_3$ (60 nm), film 2: compound **4**: PVK (1:2, 5 wt % in $CHCl_3$) (60 nm)] were measured using a Jobin Yvon FL3-212-TCSPC fluorospectrophotometer. With an excitation laser source of 340 nm, all the PL transient decay curves of films were monitored at 430 nm. The photoluminescence quantum yield data were obtained using rhodamine B as standard.[26]

4.4. Device fabrication and characterisation

All devices were prepared on patterned indium tin oxide (ITO) coated glass substrate with a sheet resistance of 20 Ω/square. The substrates were treated in an ultraviolet-ozone chamber after the following pre-clean procedure: ultrasonically cleaned with detergent, acetone, ethanol and deionised water. The hole transport polymer PEDOT:PSS was spin-coated with a thickness of 50 nm. After heat treatment, the emitting polymer consisting of PVK doped

with compound **4** and OXD-7 at the optimal weight ratio of [12:7:3 w/w] in a concentration of 10 mg/ml $CHCl_3$ solution was spin-coated at 1200 rpm (low speed) for 5 s and at 4000 rpm (high speed) for 30 s, respectively, which resulted in a film thickness of 80 nm. The ITO substrate coated with PEDOT:PSS and the emitting layer was cured on a hot plate in a glove box to remove solvent at 100 °C for 30 min. Then Bphen, LiF and Al was deposited onto the above substrate sequentially without breaking the vacuum environment at a base pressure $<2\times10^{-4}$ Pa. The evaporation rates were 0.2 nm/s, 0.07 nm/s and 1 nm/s for the organic layer, LiF layer and Al cathode, respectively. An active emitting area of 3×3 mm^2 was determined by a shadow mask. The current–voltage–luminance (J–V–L) characteristics were recorded with a PR650 spectra scan spectrometer and a Keithley 2400 programmable voltage–current source. The electroluminescent spectra, CIE coordinates and CRI of the devices were measured using a PR650 spectra scan spectrometer. All the measurements were carried out in ambient atmosphere at room temperature.

Acknowledgements

This work was supported by the National Natural Science Foundation of China (Grant No. 60906022), Scientific Developing Foundation of Tianjin Education Commission, China (Grant No. 2011ZD02), and Tianjin Natural Science Council (Grant No. 10SYSYJC28100). The UK authors acknowledge the support of EPSRC.

Supplementary data

Supplementary data related to this article can be found at http://dx.doi.org/10.1016/j.tet.2014.01.073.

References and notes

1. Grimsdale, A. C.; Chan, K. L.; Martin, R. E.; Jokisz, P. G.; Holmes, A. B. *Chem. Rev.* **2009**, *109*, 897.
2. Prachumrak, N.; Namuangruk, S.; Keawin, T.; Jungsuttingwong, S.; Sudyoadsuk, T.; Promarak, V. *Eur. J. Org. Chem.* **2013**, 3825.
3. (a) Reineke, S.; Lindner, F.; Schwartz, G.; Seidler, N.; Walzer, K.; Lüssem, B.; Leo, K. *Nature* **2009**, *459*, 234; (b) McCarthy, M. A.; Liu, B.; Donoghue, E. P.; Kravchenko, I.; Kim, D. Y.; So, F.; Rinzler, A. G. *Science* **2011**, *332*, 570; (c) Kamtekar, K. T.; Monkman, A. P.; Bryce, M. R. *Adv. Mater.* **2010**, *22*, 572; (d) Farinola, G. M.; Ragni, R. *Chem. Soc. Rev.* **2011**, *40*, 3467; (e) Sasabe, H.; Kido, J. *J. Mater. Chem. C* **2013**, *1*, 1699.
4. Kido, J.; Kimura, M.; Nagai, K. *Science* **1995**, *267*, 1332.
5. Gather, M. C.; Kohnen, A.; Meerholz, K. *Adv. Mater.* **2011**, *23*, 233.
6. D'Andrade, B. W.; Holmes, R. J.; Forrest, S. R. *Adv. Mater.* **2004**, *16*, 624.
7. Sun, Y.; Giebink, N. C.; Kanno, H.; Ma, B.; Thompson, M. E.; Forrest, S. R. *Nature* **2006**, *440*, 908.
8. Lee, K. H.; Son, C. S.; Lee, J. Y.; Kang, S.; Yook, K. S.; Jeon, S. O.; Lee, J. Y.; Yoon, S. S. *Eur. J. Org. Chem.* **2011**, 4708.
9. (a) Al Attar, H. A.; Monkman, A. P.; Tavasli, M.; Bettington, S.; Bryce, M. R. *Appl. Phys. Lett.* **2005**, *86*, 121101; (b) Sasabe, H.; Takamatsu, J.-I.; Motoyama, T.; Watanabe, S.; Wagenblast, G.; Langer, N.; Molt, O.; Fuchs, E.; Lennartz, C.; Kido, J. *Adv. Mater.* **2010**, *22*, 5003; (c) Yang, X.; Zhao, Y.; Zhang, X.; Li, R.; Dang, J.; Li, Y.; Zhou, G.; Wu, Z.; Ma, D.; Wong, W.-Y.; Zhao, X.; Ren, A.; Wang, L.; Hou, X. *J. Mater. Chem.* **2012**, *22*, 7136; (d) Wan, J.; Zheng, C.-J.; Fung, M.-K.; Liu, X.-K.; Lee, C.-S.; Zhang, X.-H. *J. Mater. Chem.* **2012**, *22*, 4502.
10. (a) Feng, J.; Li, F.; Gao, W.; Liu, S.; Liu, Y.; Wang, Y. *Appl. Phys. Lett.* **2001**, *78*, 3947; (b) Adamovich, V.; Brooks, J.; Tamayo, A.; Alexander, A. M.; Djurovich, P. I.; D'Andrade, B. W.; Adachi, C.; Forrest, S. R.; Thompson, M. E. *New J. Chem.* **2002**, *26*, 1171; (c) Liu, Y.; Guo, J.; Zhang, H.; Wang, Y. *Angew. Chem., Int. Ed.* **2002**, *41*, 182; (d) Liu, Y.; Nishiura, M.; Wang, Y.; Hou, Z. *J. Am. Chem. Soc.* **2006**, *128*, 5592; (e) Williams, E. L.; Haavisto, K.; Li, J.; Jabbour, G. E. *Adv. Mater.* **2007**, *19*, 197; (f) Fleetham, T.; Ecton, J.; Wang, Z.; Bakken, N.; Li, J. *Adv. Mater.* **2013**, *25*, 2573.
11. (a) Li, J. Y.; Liu, D.; Ma, C.; Lengyel, O.; Lee, C.-S.; Tung, C.-H.; Lee, S. *Adv. Mater.* **2004**, *16*, 1538; (b) Mazzeo, M.; Vitale, V.; Della Sala, F.; Anni, M.; Barbarella, G.; Favaretto, L.; Sotgiu, G.; Cingolani, R.; Gigli, G. *Adv. Mater.* **2005**, *17*, 34; (c) Zhao, Z.; Xu, B.; Yang, Z.; Wang, H.; Wang, X.; Lu, P.; Tian, W. *J. Phys. Chem. C* **2008**, *112*, 8511; (d) Tao, S.; Zhou, Y.; Lee, C.-S.; Lee, S.-T.; Huang, D.; Zhang, X. *J. Mater. Chem.* **2008**, *18*, 3981; (e) Liu, L.; Chen, F.; Xu, B.; Dong, Y.; Zhao, Z.; Tian, W.; Ping, L. *Synth. Met.* **2010**, *160*, 1968.
12. (a) Liu, J.; Zhou, Q.; Cheng, Y.; Geng, Y.; Wang, L.; Ma, D.; Jing, X.; Wang, F. *Adv. Funct. Mater.* **2006**, *16*, 957; (b) Luo, J.; Li, X.; Hou, Q.; Peng, J.; Yang, W.; Cao, Y. *Adv. Mater.* **2007**, *19*, 1113.
13. (a) Iraqi, A.; Pickup, D. F.; Yi, H. *Chem. Mater.* **2006**, *18*, 1007; (b) Lo, S.-C.; Burn, P. L. *Chem. Rev.* **2007**, *107*, 1097.
14. Review: Hughes, G.; Bryce, M. R. *J. Mater. Chem.* **2005**, *15*, 94.
15. (a) Guan, M.; Bian, Z. Q.; Zhou, Y. F.; Li, F. Y.; Li, Z. J.; Huang, C. H. *Chem. Commun.* **2003**, 2708; (b) Thomas, K. R. J.; Lin, J. T.; Tao, Y.-T.; Chuen, C.-H. *Chem. Mater.* **2004**, *16*, 5437; (c) Fisher, A. L.; Linton, K. E.; Kamtekar, K. T.; Pearson, C.; Bryce, M. R.; Petty, M. C. *Chem. Mater.* **2011**, *23*, 1640; (d) Linton, K. E.; Fisher, A. L.; Pearson, C.; Fox, M. A.; Pålsson, L.-O.; Bryce, M. R.; Petty, M. C. *J. Mater. Chem.* **2012**, *22*, 11816.
16. Wang, C.; Pålsson, L.-O.; Batsanov, A. S.; Bryce, M. R. *J. Am. Chem. Soc.* **2006**, *128*, 3789.
17. Adhikari, R. M.; Mondal, R.; Shah, B. K.; Neckers, D. C. *J. Org. Chem.* **2007**, *72*, 4727.
18. Pålsson, L.-O.; Wang, C.; Batsanov, A. S.; King, S. M.; Beeby, A.; Monkman, A. P.; Bryce, M. R. *Chem.—Eur. J.* **2010**, *16*, 1470.
19. Brinkmann, M.; Gadret, G.; Muccini, M.; Taliani, C.; Masciocchi, N.; Sironi, A. *J. Am. Chem. Soc.* **2000**, *122*, 5147.
20. Thomas, K. R. J.; Lin, J. T.; Tao, Y.-T.; Chuen, C.-H. *Chem. Mater.* **2002**, *14*, 3852.
21. Steinbacher, F. S.; Krause, R.; Hunze, A.; Winnacker, A. *Phys. Status Solidi A* **2012**, *209*, 340.
22. Jankus, V.; Monkman, A. P. *Adv. Funct. Mater.* **2011**, *21*, 3350.
23. Xu, Y. H.; Peng, J. B.; Jiang, J. X.; Xu, W.; Yang, W.; Cao, Y. *Appl. Phys. Lett.* **2005**, *87*, 193502-1.
24. Kondakov, D. Y. *J. Appl. Phys.* **2006**, *99*, 024901-1.
25. Hou, L. D.; Duan, L.; Qiao, J.; Li, W.; Zhang, D. Q.; Qiu, Y. *Appl. Phys. Lett.* **2008**, *92*, 263301-1.
26. Brouwer, A. M. *Pure Appl. Chem.* **2011**, *83*, 2213.